Polymer Journal (2019) 51:771–780
https://doi.org/10.1038/s41428-019-0191-6

ORIGINAL ARTICLE

Oligopeptide-side chained alginate nanocarrier for melittin-targeted chemotherapy

Karnthidaporn Wattanakul[1] · Toyoko Imae[1,2] · Wen-Wei Chang[3] · Chih-Chien Chu[4,5] · Rina Nakahata[6] · Shin-ichi Yusa[6]

Received: 22 January 2019 / Revised: 23 March 2019 / Accepted: 25 March 2019 / Published online: 10 May 2019

Abstract

A melittin-targeting drug carrier was successfully synthesized by the grafting of sodium alginate to an oligopeptide via an amidation method at different oligopeptide:alginate unit molar ratios. The average sizes of the oligopeptide–alginate nanoparticles formed in the presence of 1 mM $CaCl_2$ decreased with increasing oligopeptide contents, indicating intramolecular interactions between oligopeptide-side chains. While the doxorubicin-loading efficiency on nanoparticles (0.1:1) was similar to that of alginate nanoparticles, the melittin-loading onto oligopeptide–alginate nanoparticles (0.1:1) was more than double that onto alginate nanoparticles, suggesting the specific interaction of melittin with the oligopeptide-side chain in the oligopeptide–alginate nanoparticles. While 2.5 μM free melittin caused almost no damage to Caco-2 cells, more than 80% of cells did not survive under the dose of 2.5 μM melittin-loaded oligopeptide–alginate nanoparticles. The results confirm that the derivation of an oligopeptide-side chain in alginate offers a specific binding site for melittin and effectively works in cancer chemotherapy.

Introduction

Chemotherapy has been a mainstay of cancer treatment for decades. However, most conventional chemotherapeutic drugs are toxic to healthy cells, and others have difficulty in penetrating cytotoxicity-inducing tumors. Therefore, targeted drug delivery is the preferred method for drug administration, which is a very promising alternative to increase the concentration of a drug at the desired target site without destroying other normal tissues [1, 2]. This function leads to a special focus on nanomedicine, because nanoparticles have a larger surface area-to-volume ratio, resulting in a greater efficiency in drug delivery and a better penetrating ability [3–5]. In cancer treatment, nanoparticles have been developed to satisfy an enhanced permeability and retention (EPR) effect to passively target tumor tissues and to increase the capability to realize active targeting through the incorporation of ligands [6–8]. Accordingly, various polymeric materials can be used to develop nanoparticle carriers, because polymeric nanoparticles can protect drugs from rapid metabolism and selectively accumulate in tumor tissues via the EPR effect.

Alginate has attracted much attention as a delivery carrier for cancer therapy due to its significant biological properties, such as biocompatibility, low immunogenicity, nontoxicity, and water-solubility. Furthermore, alginate is a

✉ Toyoko Imae
imae@mail.ntust.edu.tw

✉ Chih-Chien Chu
jrchu3933@gmail.com

[1] Graduate Institute of Applied Science and Technology, National Taiwan University of Science and Technology, Keelung Road, Taipei 10607, Taiwan

[2] Department of Chemical Engineering, National Taiwan University of Science and Technology, Keelung Road, Taipei 10607, Taiwan

[3] Department of Biomedical Sciences, Chung Shan Medical University, Jianguo North Road, Taichung 40201, Taiwan

[4] Department of Medical Applied Chemistry, Chung Shan Medical University, Jianguo North Road, Taichung 40201, Taiwan

[5] Department of Medical Education, Chung Shan Medical University Hospital, Taichung 40201, Taiwan

[6] Department of Materials Science and Chemistry, University of Hyogo, Himeji, Hyogo 671-2280, Japan

linear anion polysaccharide composed of alternating blocks of 1,4-linked hexuronic acid residues, namely, β-D-mannuronate (M) and α-L-glucuronate (G) residues, which possess specific structures and show pH-dependent swelling behavior. The carboxyl group transforms from the protonated state to the deprotonated state at around pH ~5, which allows the neutral polymer to shrink at acidic pH values and the charged polymer to swell in at neutral or basic pH values. However, low encapsulation efficiency and fast release of drugs have been observed for alginate microcapsules [9, 10].

Melittin, a major peptide constituent of bee venom, is a potential anticancer candidate, because cancer cells are less likely to develop resistance to a membrane pore former. Thus, melittin has the ability to induce cell cycle arrest, growth inhibition, apoptosis, and necrosis in various cancer cells [11–13]. The chemical formula of melittin is $C_{131}H_{228}N_{38}O_{32}$, and it consists of the known 26 amino acid sequence, Gly-Ile-Gly-Ala-Val-Leu-Lys-Val-Leu-The-Thr-Gly-Leu-Pro-Ala-Leu-Ile-Ser-Trp-Ile-Lys-Arg-Lys-Arg-Gln-Gln [14, 15].

Therefore, in this study, oligopeptide-side chained alginate nanoparticles were synthesized from water-soluble alginate and oligopeptides of α-alanine to obtain melittin-targeted drug delivery. In detail, we introduced an oligopeptide side chain with a propylamine terminal as the blocking group of the c-terminal of the oligopeptide. The oligopeptide side chain provides an effective binding site of melittin to be the oligopeptide. Hydrogen bonding is an attractive force by which drugs can be retained in drug delivery systems, but at the same time, these forces become weak and can release drugs at higher temperatures. The physicochemical characteristics of oligopeptide-side chain alginate nanoparticles were determined using nuclear magnetic resonance (NMR), Fourier-transform infrared (FTIR) absorption spectroscopy, and static and dynamic light scattering (SLS and DLS). The characteristics of action as drug carriers were compared between melittin and doxorubicin (DOX). The specific effectivity of the oligopeptide side chain in melittin delivery was discussed in association with cell viability.

Materials and methods

Reagents

Sodium alginate (SA, 216.12 g/unit mol, weight-average molecular weight 1.65×10^5 g/mol, weight-average polymerization degree 763), N-hydroxysuccinimide (NHS), and 1-(3-dimethylaminopropyl)-3-ethylcarbodiimide (EDC) were purchased from Acros (Belgium), and *tert*-butoxycarbonyl (BOC)-alanine was obtained from the Protein Research Foundation (Japan). Melittin and DOX hydrochloride were supplied by Sigma-Aldrich (USA). All other chemical reagents obtained from commercial sources and used in the study were of analytical grade.

Synthesis of alginate with an oligopeptide-side chain (oligopeptide–alginate)

The synthesis of oligopeptide–alginate was performed through four steps, as illustrated in Scheme 1. In the first step, to 1 mmol of BOC-alanine (compound (1)) dissolved in dimethylformamide (DMF), equimolar amounts of NHS and EDC were added under continuous stirring,

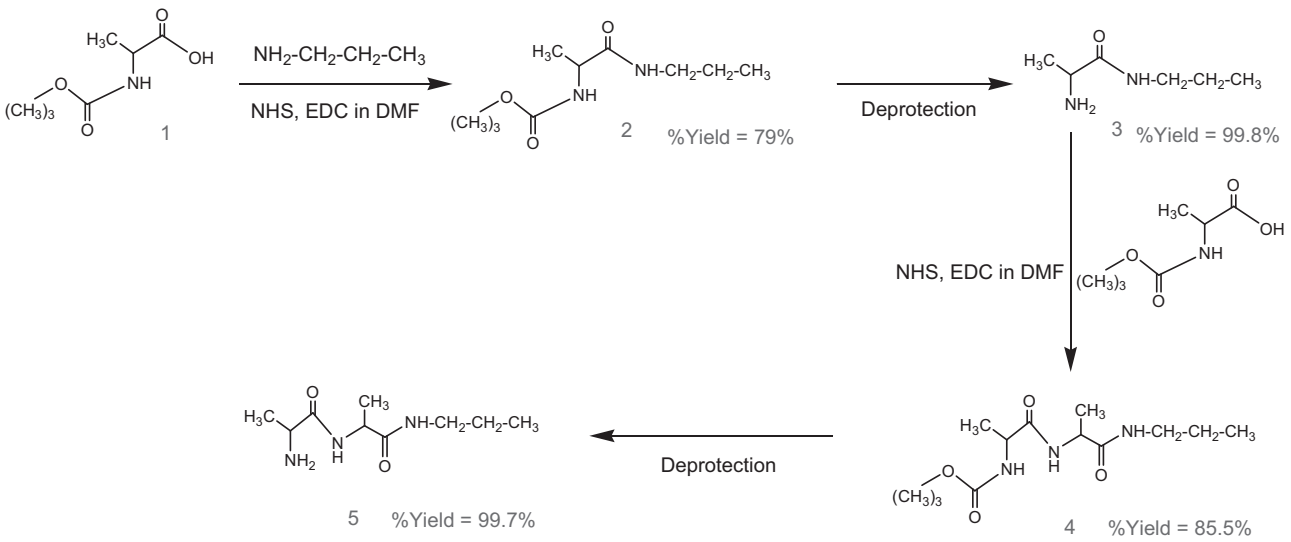

Scheme 1 Synthesis processes of oligopeptide

and then equimolar propylamine was added to the mixture. After the mixture was stirred at room temperature for 24 h, the solution was added into a mixture of diethyl ether and hexane (1:1 by volume) to precipitate the compound (2). The collected compound (2) was reserved for the second step.

The BOC terminal of compound (2) was deprotected using 5 M HCl in isopropanol. The solution was stirred at 50 °C for 4 h, and the pH of the solution was adjusted to pH 7–8 using a saturated $NaHCO_3$ solution at the end of the reaction. After the solution was cooled to 20 °C, the organic solvent phase was collected and added to a mixture of diethyl ether and hexane (1:1 by volume) to precipitate and obtain the required compound (3).

To prepare the Ala–Ala dipeptide, BOC-alanine was reacted with compound (3) using an amidation method in DMF. 1 mmol of NHS and an equimolar amount of EDC were added into the BOC-alanine solution, and then compound (3) was added. The solution was continuously stirred at room temperature for 24 h. Then, the solution was poured into a mixture of diethyl ether and hexane (1:1 by volume) to obtain compound (4).

In the last step, to obtain the required compound (5), the BOC terminal of compound (4) was deprotected by the same procedure as that used for the production of compound (3). The yield of each step is described in Scheme 1. The yield was always high enough.

The obtained oligopeptide was further used to prepare the oligopeptide–alginate by an amidation method in DMF, as shown in Scheme 2. First, 1 mmol of NHS and an equimolar amount of EDC were added into the alginate solution, and then compound (5) was added at various molar ratios (0.033:1, 0.05:1, and 0.1:1 molar ratios of oligopeptide molecule:alginate repeating unit). The solution was continuously stirred at room temperature for 24 h. Then, the solution was poured into the mixture of diethyl ether and hexane (1:1 by volume) to obtain the oligopeptide–alginate. ^{1}H-NMR (600 MHz, D_2O, oligopeptide): 1.12, 1.80, 3.05, 3.17, 3.26 ppm (CH_3(terminal), CH_2, CH_2, CH_3, CH_3), 3.63 ppm (alginate).

Preparation of alginate and oligopeptide–alginate nanoparticles

To obtain calcium ion-induced alginate nanoparticles, sodium alginate solutions at different concentrations (0.01, 0.075, and 0.1 mg/ml) were prepared by dissolving proper amounts of sodium alginate powder in water at 30 °C. Then, 50 µl of 0.02 M $CaCl_2$ was dropwise added to the stirred aqueous solution (1 ml) of sodium alginate, and the mixture was continuously stirred for 2 h at 30 °C. Then, the concentration of $CaCl_2$ in the prepared solution was 1 mM.

Correspondingly, an oligopeptide–alginate solution at a concentration of 0.1 mg/ml was prepared by dissolving oligopeptide–alginate powder in water at 30 °C. Then, 50 µl of 0.02 M $CaCl_2$ was dropwise added to the stirred aqueous solution (1 ml) of oligopeptide–alginate, and the solution was continuously stirred for 2 h at 30 °C.

Characterization

The ^{1}H-NMR measurement was performed at room temperature on an AVANCE III HD600 NMR spectrometer (Bruker) using a 5 mm NMR tube. The alginate and oligo-alginate were dissolved in D_2O (99.9%) to a concentration of 10 mg/ml. The FT-IR absorption spectra on KBr disks

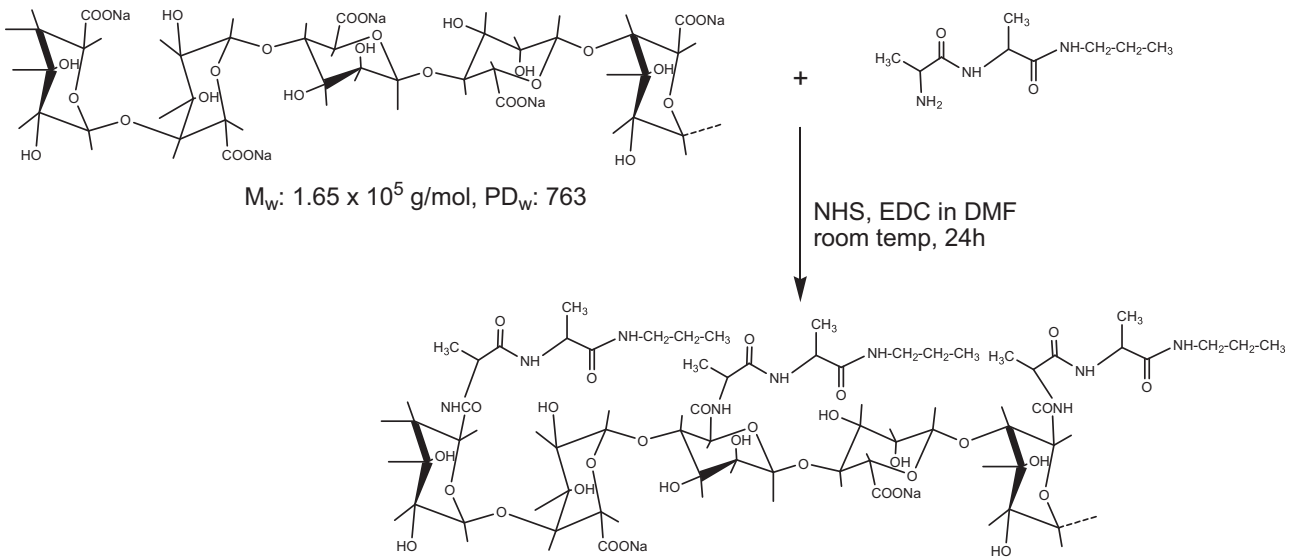

Scheme 2 Synthesis process of oligopeptide–alginate

were recorded using a Thermo Scientific Nicolet 6700 FTIR spectrophotometer with 64 scans (resolution = 4 cm^{-1}).

The static light scattering (SLS) measurement was performed at 25 °C on an Otsuka Electronics Photal DLS-7000 (Japan) equipped with a He–Ne laser (10 mW at 633 nm) as a light source. The weight-average molecular weight (M_w) and z-average radius of gyration (R_g) were evaluated from the Debye plot. The refractive index increment against the concentration (dn/dC_p) at 633 nm was measured at 25 °C on an Otsuka Electronics Photal DRM-3000 (Japan). Sample solutions were filtered with a 0.2 µm-pore size membrane filter. The surface charge and particle size were determined by measuring the zeta potential and DLS using a Malvern Nano-ZS90 (Japan) with a He–Ne laser beam at 633 nm and 25 °C. The value was recorded as the average of three measurements.

Loading and release of drugs on alginate and oligopeptide–alginate nanoparticles

To load drugs into alginate and oligopeptide–alginate nanoparticles, aqueous solutions of DOX (500 µl) or melittin (100 µl) at different concentrations of 1–100 µg/ml were incubated with an aqueous solution (1 ml) of alginate or oligopeptide–alginate. All solutions were gently stirred at room temperature for 24 h in the dark. Then, 50 µl of 0.02 M $CaCl_2$ were dropwise added to the stirred aqueous mixture and then continuously stirred for 2 h at 30 °C under dark conditions.

The drug-loaded nanoparticle solutions were dialyzed in a cellulose tubular membrane (MWCO of 6000–8000 g/mol) against water for 72 h to remove the unbound drug. The amount of unbound drug in the dialyzed outer solution was determined quantitatively from the absorbance at the band (485 nm) of DOX or the band (280 nm) of melittin using a calibration curve. The amount of loaded drug was evaluated by subtracting the amount of unbound drug from the initial amount of drug.

The controlled release of drugs was examined in phosphate buffered saline (PBS) at pH 5.5 and 7.4. A nanoparticle solution in a dialysis membrane (MWCO = 3500 g/mol) was dialyzed in 10 ml of water under constant stirring for 72 h at room temperature. The concentration of drugs released into water from the nanoparticle solution was quantified using the absorbance at the band of 485 nm for DOX and of 280 nm for melittin.

Cell viability of alginate and oligopeptide–alginate nanoparticles

Caco-2 cells were obtained from the American Type Culture Collection (ATCC, Manassas, VA) and cultured in DMEM medium (Life Technologies Corporation) supplemented with 10% fetal bovine serum (Life Technologies Corporation), bovine insulin (5 µg/ml, Sigma-Aldrich), sodium pyruvate (1 mM, Biological Industries), antibiotics (100 unit/ml penicillin and 100 µg/ml streptomycin, Life Technologies Corporation), and Glutamax (2 mM, Life Technologies Corporation). The cells were then seeded into a 96-well plate at a density of 1×10^4 cells per well. After incubation for 24 h, the sample solutions were added into each well to attain the desired concentrations. After incubation at 37 °C for 48 h, a solution of 2-(4-iodophenyl)-3-(4-nitrophenyl)-5-(2,4-disulfophenyl)-2H-tetrazolium salt (WST-1) was added at 10 µl/well, and the mixture was incubated at 37 °C for another 3 h. The viability of the cells was determined by the visible absorbance at 440 nm after subtracting the reference absorbance at 650 nm using an ELISA microplate reader (EZ Read 400, Biochrom Ltd., Cambridge, UK). Three independent experiments were performed, and each experiment was done in triplicate.

Results and discussion

Characterization of the oligopeptide–alginate nanoparticles

Alanine dipeptides were synthesized by using BOC-alanine as a starting material. Figure 1 shows the FT-IR absorption spectra of compounds 1–5, the chemical structures of which are illustrated in Scheme 1. The absorption band of BOC-alanine (compound (1)) observed at 3350 cm^{-1} can be assigned to the NH and OH stretching vibration modes, and the absorption bands observed at 1717 and 1699 cm^{-1} can be assigned to the C=O stretching vibration mode of the urethane and carboxylic acid groups. After the reaction of BOC-alanine with trimethylamine, new absorption bands were observed at 1652 and 1562 cm^{-1}, assigned to the amide I and

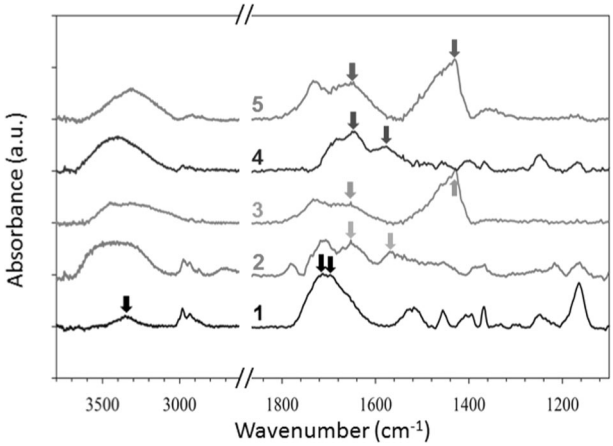

Fig. 1 FT-IR absorption spectra of compounds 1–5

amide II modes of compound (2), respectively [16–19]. After the deprotection of BOC to obtain compound (3), absorption bands were observed at 1655 and 1432 cm^{-1}, which were assigned to the C=O stretching and NH_2 bending vibration modes of the alanine dipeptide. Similar variation bands on IR absorption spectra occurred even during the process of the syntheses of compounds (4) and (5), wherein amidation and deprotection reactions, respectively, were performed. Thus, similar bands to those of compounds (2) and (3) were obtained at 1650 and 1580 cm^{-1} for compound (4) and at 1652 and 1439 cm^{-1} for compound (5).

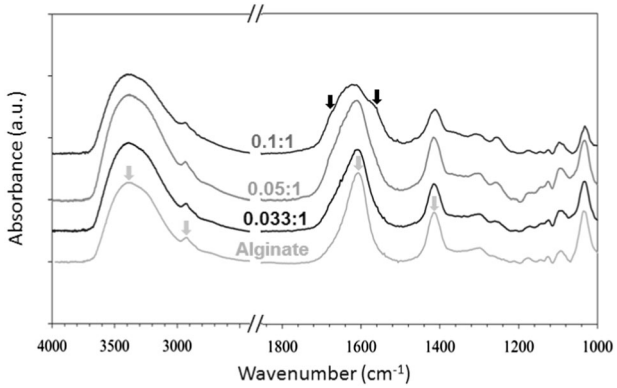

Fig. 2 FT-IR absorption spectra of alginate and oligopeptide–alginates

The oligopeptide–alginates with different molar ratios (0.033:1, 0.05:1, and 0.1:1) of the oligopeptide relative to the alginate chain unit were prepared. Figure 2 shows the IR absorption spectra of alginate and the oligopeptide–alginates. The characteristic IR bands of alginate appeared at 3410, 1608, and 1418 cm^{-1} and were attributed to the O–H stretching and carboxylate antisymmetrical and symmetrical stretching vibration modes, respectively. A small band at 2940 cm^{-1} could be assigned to the C–H stretching vibration mode. While these characteristic bands of alginate can also be observed for oligopeptide–alginates, additional shoulder bands at 1680 and 1560 cm^{-1} were observed for the oligopeptide–alginates. These bands could be assigned to the amide I and II modes, respectively, of the oligopeptide [20, 21], and these shoulders were clearly observed when the molar ratio of oligopeptide to alginate was 0.1:1.

The successful modification of alginate was also confirmed by ^{1}H-NMR. In Fig. 3, the proton chemical shift at 3.63 ppm can be assigned to the proton of alginate.

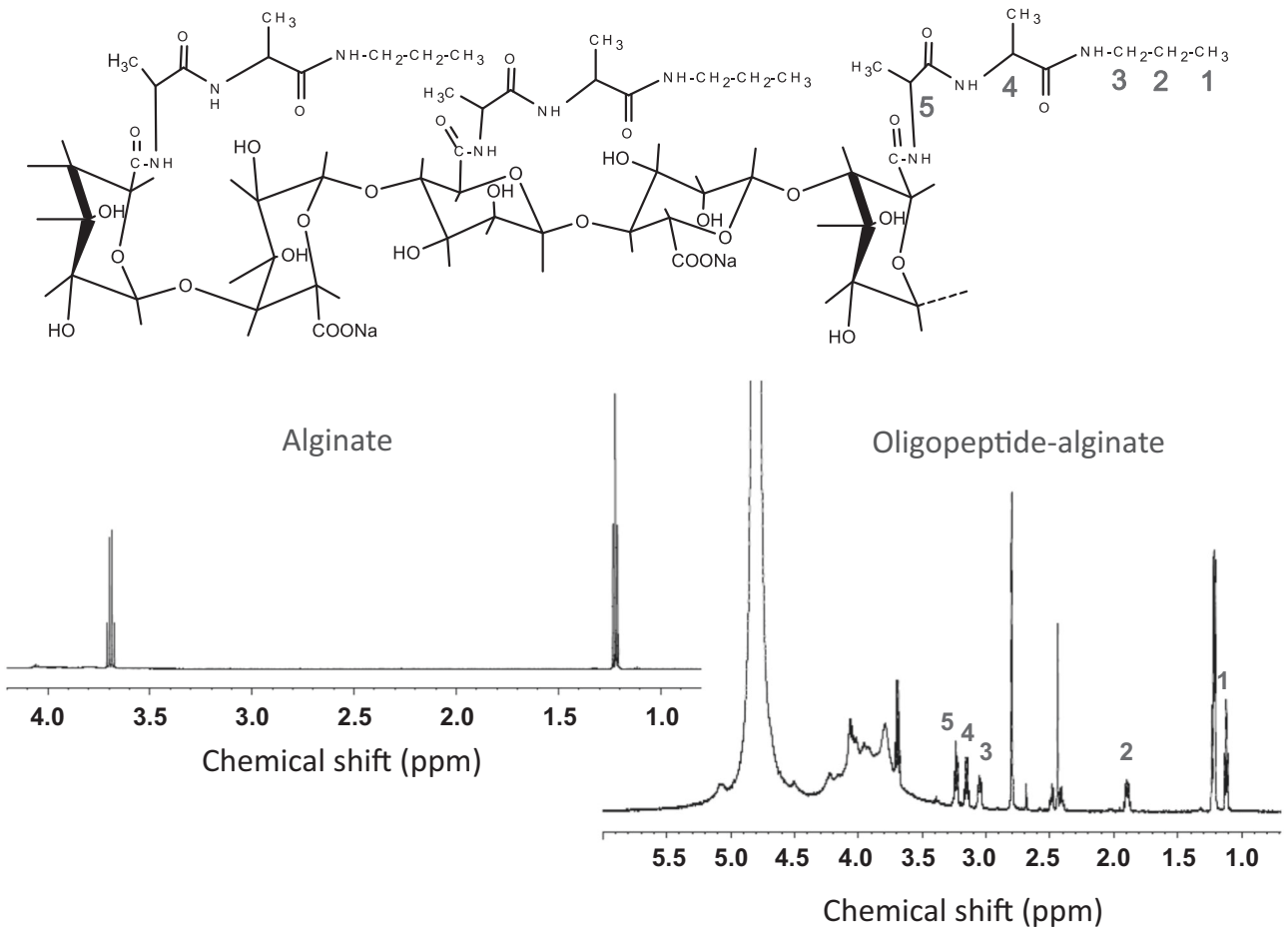

Fig. 3 ^{1}H-NMR spectra of alginate and oligopeptide–alginate(0.1:1)

Table 1 Weight-average molecular weights (M_w), *z*-average radii of gyration (R_g), hydrodynamic radii (R_h), and refractive index increment against concentration (dn/dC_p) for alginate and oligopeptide–alginate(0.1:1) (0.1 mg/ml) in aqueous 0.01 M NaCl solution at pH 9 and for oligopeptide–alginate(0.1:1) (0.1 mg/ml) in aqueous 1 mM $CaCl_2$ solution

	$M_w \times 10^5$ (g/mol)	R_g (nm)	R_h (nm)	R_g/R_h	dn/dC_p (ml/g)
Alginate in NaCl	1.65	66.5	44.2	1.50	0.155
Oligopeptide–alginate(0.1:1) in NaCl	2.02	96.3	84.2	1.14	0.179
Oligopeptide–alginate(0.1:1) in $CaCl_2$	75.6	149			0.103

However, additional proton chemical shifts of the oligopeptide–alginate (at 0.1:1) were observed below this chemical shift and were assigned to the methyl, methylene and Cα protons of the oligopeptide. Additionally, Fig. 3 exhibits a signal related to the presence of the proton of the amide group at 4.88 ppm [22].

Sizes of alginate and oligopeptide–alginate nanoparticles

The weight-average molecular weight (M_w), hydrodynamic radius (R_h), and *z*-average radius of gyration (R_g) were evaluated from SLS and DLS measurements performed for alginate and oligopeptide–alginate(0.1:1) (0.1 mg/ml) in aqueous 0.01 M NaCl solutions at pH 9. The light scattering data, M_w and R_g, obtained from extrapolation of the Debye plot to the scattering angle $(\theta) \rightarrow 0°$ and the slope of the Debye plot, respectively, are summarized in Table 1, along with the values of R_h and the refractive index increment (dn/dC_p, C_p is the polymer concentration). The polymerization degree of alginate estimated from the M_w value was 763, and the increase in the molecular weight of the oligopeptide–alginate is attributed to the substitution of alginate monomer units by the oligopeptide. The R_g/R_h values were 1.50 and 1.14, suggesting that the polydispersity of oligopeptide–alginate(0.1:1) was less than that of alginate. The density (*d*) calculated from M_w and R_h was 0.76 and 0.13 mg/cm^3, respectively, for alginate and oligopeptide–alginate(0.1:1). These small *d* values indicate that the aggregates contained a large amount of water, and this characteristic is advantageous for loading small molecules such as drugs. The SLS measurement was performed for oligopeptide–alginate(0.1:1) in an aqueous 1 mM $CaCl_2$ solution. The increase of the M_w and R_g values (see Table 1) indicates the agglomeration of oligopeptide–alginate(0.1:1). The calculated aggregation number was 37.

The hydrodynamic sizes ($2R_h$) from DLS in aqueous solutions in the absence and presence of 1 mM $CaCl_2$ were measured for alginate and oligopeptide–alginates at different oligopeptide:alginate unit molar ratios. The sizes (685–724 nm in water and 201–248 nm in 1 mM $CaCl_2$) of alginate were almost independent of the alginate concentration (0.01–0.1 mg/ml), although the alginate size in water was shrunk by approximately 1/3 after adding 1 mM $CaCl_2$. These results are not amazing, if ionic crosslinkage occurs. The sodium alginate molecules were crosslinked in the presence of Ca ions due to the coupling of Ca ions with two carboxylate ions in an alginate molecule [23]. Thus, alginate molecules in $CaCl_2$ solution cannot expand by electrostatic repulsion between free carboxylates, which happened in the solutions without $CaCl_2$. It can be noted that such size variation of alginate depends on the kind of added salt but does not depend on the alginate concentration.

The average sizes of the oligopeptide–alginate nanoparticles in aqueous 1 mM $CaCl_2$ solution evaluated through DLS were 296, 180, 125, and 54 nm at different oligopeptide:alginate unit molar ratios (0:1, 0.033:1, 0.05:1, and 0.1:1, respectively), indicating the decrease of particle size with increasing oligopeptide content. This can be attributed to the lesser negative charge on the alginate chain after reaction of the carboxyl group on the alginate with the amine group of the oligopeptide, leading to less repulsion within the alginate chain [24]. Another possible cause is the interaction between oligopeptide side chains in the oligopeptide–alginates. This phenomenon is largely possible, because oligopeptides can form β-sheets through hydrogen bonding [25, 26].

As shown in Fig. 4a, the zeta potential of both alginate and oligopeptide–alginate(0.1:1) nanoparticles in aqueous 1 mM $CaCl_2$ solution was neutral in acidic media and negative (−34 to −36 mV) under neutral and alkaline (pH 6–11) conditions, because all carboxyl groups in the alginate and oligopeptide–alginate are protonated in acidic media and deprotonated, becoming negatively charged on the particle surface, under neutral and alkaline conditions, although the p*K*a values of the carboxyl group were 4.1 and 3.2, respectively, for the alginate and oligopeptide–alginate (0.1:1).

In addition, it can be known from Fig. 4b that changing the pH in aqueous solution also affects the hydrodynamic particle size of the nanoparticles, because alginate nanogel

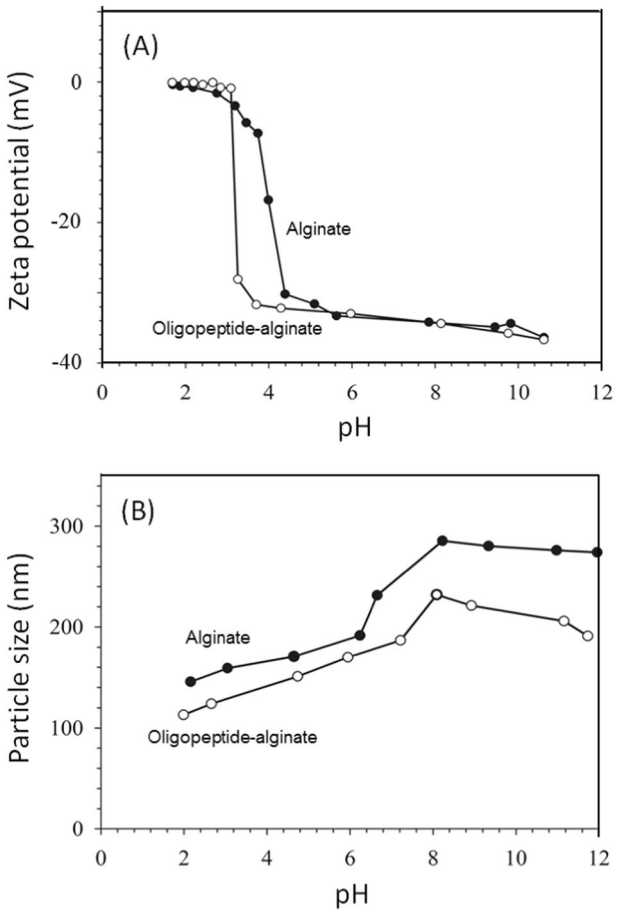

Fig. 4 The pH dependence of **a** the zeta potential and **b** the particle size of alginate and oligopeptide–alginate(0.1:1) nanoparticles

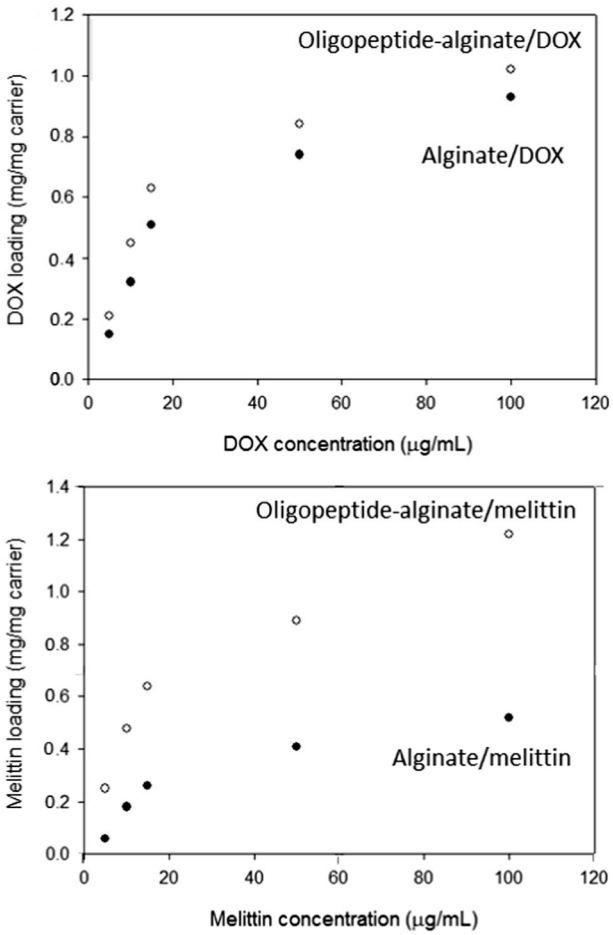

Fig. 5 (Top) DOX and (bottom) melittin loading onto alginate and oligopeptide–alginate(0.1:1) nanoparticles

is a pH-responsive anionic nanoparticle. Under acidic conditions below the p*K*a (4.1) of alginate, the majority of the groups exist as COOH, which results in less electrostatic repulsion on the alginate chain. At elevated pH values, the COOH groups are deprotonated to COO^-, which increases the electrostatic repulsion among charges on the alginate chain, leading to swelling, namely, increasing the particle size of the alginate nanogels [27, 28]. Since the carboxyl groups in alginate are partly substituted by the oligopeptide side chain, the total amount of carboxyl groups on the oligopeptide–alginate is less than that of pristine alginate, and there is an additional attractive interaction between the oligopeptides, as described above. Therefore, the particle size of oligopeptide–alginate is always smaller than that of alginate. However, the pH dependence of the hydrodynamic size cannot be explained by aggregate formation, because less-charged polymers can easy aggregate due to lesser electrostatic repulsion, and vice versa. In this situation, the hydrodynamic size must be larger under acidic conditions than under alkaline conditions, and the results in Fig. 4b do not coincide with this assumption.

Drug loading and release via alginate and oligopeptide–alginate nanoparticles

To assess the effectiveness of a nanoparticle as a drug nanocarrier, the amount of drug loading is one of the evaluations used. Therefore, the loading efficiency of alginate and oligopeptide–alginate nanoparticles was evaluated by comparison between DOX and melittin. The amounts of the drugs loaded onto the nanoparticles—that is, the nanocarriers—were plotted as a function of drug concentration, as shown in Fig. 5. The results demonstrate that the drug loading onto both nanocarriers initially increased with increasing drug concentration and became saturated at higher drug concentrations for both drugs. The difference between melittin and DOX is distinct in terms of the drug loading amount. While the loading amount of DOX was only 10% higher on oligopeptide–alginate than on alginate, the melittin loading on oligopeptide–alginate was more than twice higher than that on alginate. This variance should have been due to differences between the interaction of the drugs with the nanocarriers. DOX

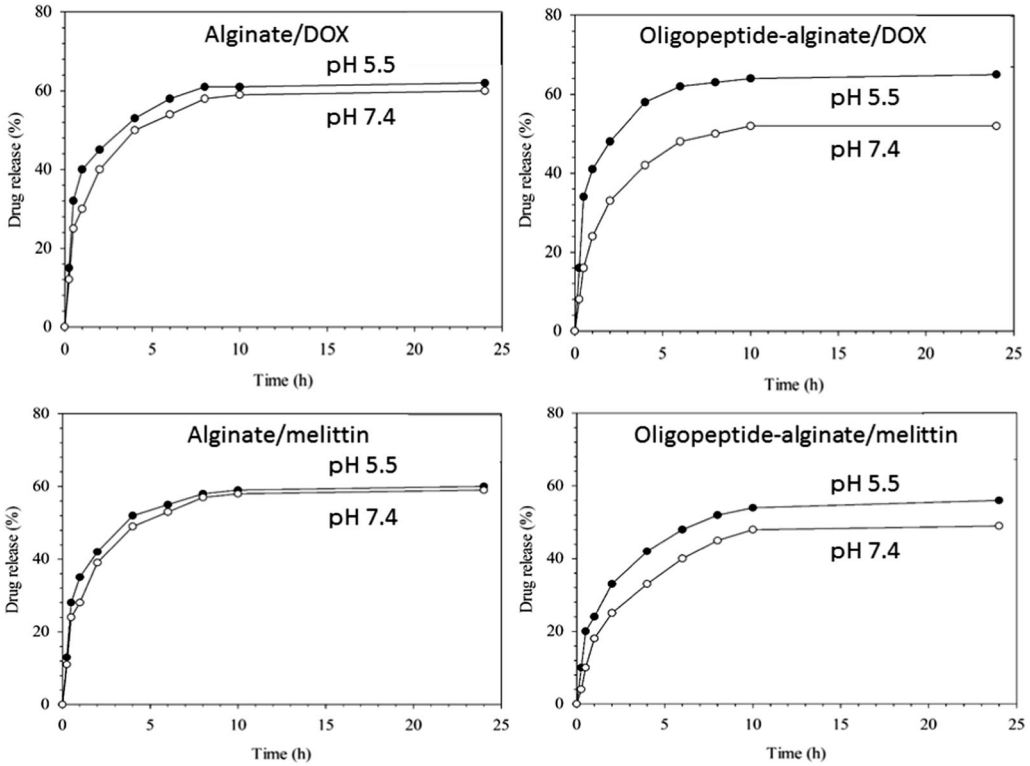

Fig. 6 Drug (DOX and melittin) release from alginate and oligopeptide–alginate nanoparticles at pH 5.5 and 7.4

Table 2 The comparison of drug loading and release (24 h, PBS) between alginate and oligopeptide–alginate nanoparticles

Carrier	DOX			Melittin		
	Loading	Release		Loading	Release	
		pH 5.5	pH 7.0		pH 5.5	pH 7.0
Alginate nanoparticle	93 (0.96)	63	60	75 (0.52)	59	58
Oligopeptide–alginate nanoparticle	96 (1.05)	65	53	98 (1.22)	52	46

Numerical values indicate efficiency (%). Numerical values in brackets are described by the unit of mg/mg carrier

loading happens mainly by interaction between the carboxylic group on the alginate structure and the amine group on DOX; thus, the difference between alginate and oligopeptide–alginate is less. In contrast, the oligopeptide-side chain in alginate induces a hydrogen bonding interaction with the peptide groups in the melittin structure, but the alginate backbone does not cause such a specific interaction with melittin.

To evaluate the in vitro drug release efficiencies of alginate and oligopeptide–alginate nanoparticles, the release of drugs from drug-loaded nanoparticles was investigated in PBS solutions at pH 5.5 and 7.4 to mimic a tumor environment and the physiological pH in body fluid, respectively [29]. As seen in Fig. 6, drug release increased as the initial time increased to 10 h and reached constant values at longer times. The saturated constant release efficiency after 24 h is listed in Table 2, along with the-loading efficiency. It should be noted that the efficiencies of both carriers and drugs were higher at pH 5.5 than at pH 7.4, and especially, the difference between the efficiency at pH 5.5 and 7.4 for both drugs was larger for oligopeptide–alginate nanoparticles than for alginate nanoparticles. These results indicate the preferable adaptability of oligopeptide–alginate nanoparticles as drug delivery carriers over alginate nanoparticles. However, the melittin release from oligopeptide–alginate nanoparticles was less than that from alginate nanoparticles and the DOX release from oligopeptide–alginate nanoparticles. It can be suggested that there is an interaction (perhaps hydrogen bonding) between the peptides in melittin and the oligopeptides in oligopeptide–alginate, resulting in less melittin released from the oligopeptide–alginate nanoparticles.

Cell viability of drug-loaded alginate and oligopeptide–alginate nanoparticles

The cytotoxicities of free DOX and DOX-loaded oligopeptide–alginate nanoparticles toward the Caco-2 cell line are shown in Fig. 7a. The results reveal that approximately 50% of cells were killed under only 0.4 μM of DOX, which is close to the effective IC50 value of this chemotherapy drug for treating gastrointestinal cells. However, using the oligopeptide–alginate as a carrier did not enhance the drug performance. In contrast, the results of cell viability after treatment with free melittin and the melittin-loaded oligopeptide–alginate carrier showed a significant difference. As seen in Fig. 7b, the oligopeptide–alginate carrier caused almost no damage to the Caco-2 cells, and more than 80% of cells survived under the dose of 2.5 μM free melittin. When an identical amount of melittin was loaded onto the oligopeptide–alginate, the hybrid nanoparticle system killed 80% of Caco-2 cells. When the concentration of melittin was increased to 5 μM, the cells were completely destroyed by both free melittin and melittin-loaded oligopeptide–alginate. The preliminary results suggest that the oligopeptide–alginate could decrease the IC50 value of melittin for Caco-2 cells, potentially making melittin loaded onto oligopeptide–alginate more effective in clinical cancer therapy.

Although the mechanism by which the alginate carrier assists the in vitro performance of the peptide drug is not established, we can speculate that the binding affinity between melittin and the oligopeptide–alginate is crucial. The driving force behind DOX (chemical drug) loading onto the oligopeptide–alginate nanoparticles is mainly physical adsorption, but melittin (peptide drug) may be adsorbed by the oligopeptide-side chains through more specific interactions (e.g., hydrogen bonding). Therefore, the cellular uptake efficiency and biodistribution of melittin could be increased by using the oligopeptide–alginate nanoparticles as the drug carrier.

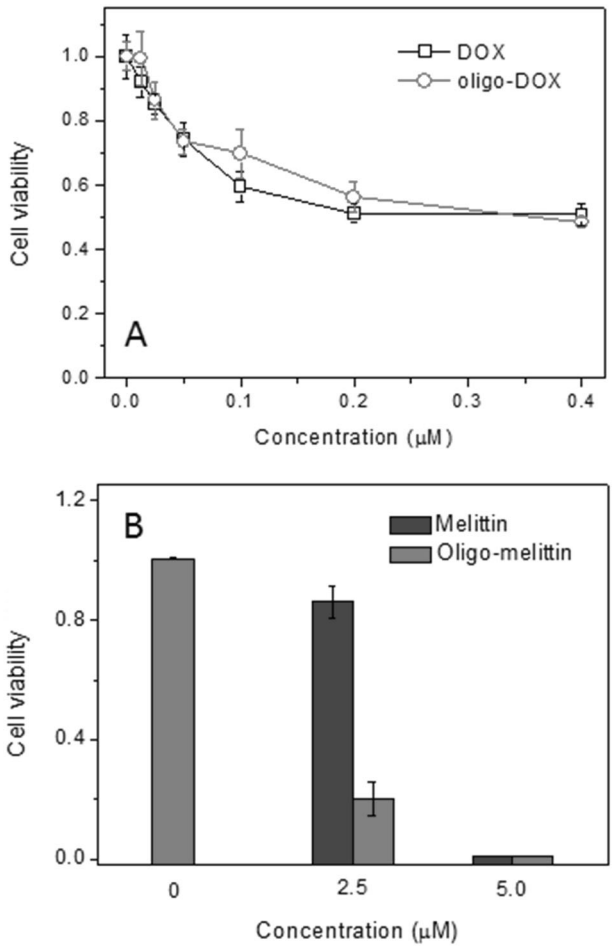

Fig. 7 In vitro cytotoxicity of **a** DOX- and **b** melittin-loaded oligopeptide–alginate nanoparticles (oligo-DOX, oligo-melittin) toward Caco-2 cells after 48 h

Conclusions

A melittin-targeting drug carrier, which possesses an oligopeptide side chain, was synthesized by the amidation reaction of sodium alginate with oligopeptide at different oligopeptide: alginate ratios. Alginate and oligopeptide–alginate nanoparticles were prepared by the addition of $CaCl_2$. The introduction of an oligopeptide side chain onto alginate had a beneficial effect on the size control of nanoparticles—the average size of the alginate nanoparticles decreased by approximately 1/4 after 10% substitution with the carboxylate moiety in alginate onto the oligopeptide, indicating interaction between oligopeptides. The hydrogen bonding interaction ability may affect the interaction with melittin, which is essentially an amphiphilic peptide. In fact, the melittin loading was superior in oligopeptide–alginate nanoparticles to that in alginate nanoparticles, in contrast to the similar DOX loading on both nanoparticles. Moreover, the viability examination also showed the excellent effectiveness of melittin-loaded oligopeptide–alginate nanoparticles in comparison with free melittin. This investigation demonstrates the advantage of oligopeptide–alginate nanoparticles as a melittin carrier and the possibility of their usage as a carrier for peptide-based drugs.

Acknowledgements This work was financially supported by the National Taiwan University of Science and Technology, Taiwan, under Grant Number 100H451201. KW appreciates the financial support from the National Taiwan University of Science and Technology, Taiwan, for postdoctoral scholarship.

Compliance with ethical standards

Conflict of interest The authors declare that they have no conflict of interest.

References

1. Ferlay J, Soerjomataram I, Ervik M, Dikshit R, Eser S, Mathers C, et al. GLOBOCAN 2012: estimated cancer incidence, mortality and prevalence worldwide in 2012 v1.0. IARC CancerBase No. 11 [Internet]. Lyon, France: International Agency for Research on Cancer. 2013;11. http://globocan.iarc.f.
2. Danhier F, Preat V. Strategies to improve the EPR effect for the delivery of anti-cancer nanomedicines. Cancer Cell Microenviron. 2015;2:1–7.
3. Cho K, Wang X, Nie S, Chen ZG, Shin DM. Therapeutic nanoparticles for drug delivery in cancer. Clin Cancer Res. 2008;14:1310–6.
4. Soni G, Yadav KS. Applications of nanoparticles in treatment and diagnosis of leukemia. Mater Sci Eng C Mater Biol Appl. 2015;47:156–64.
5. Masood F. Polymeric nanoparticles for targeted drug delivery system for cancer therapy. Mater Sci Eng C Mater Biol Appl. 2016;60:569–78.
6. Wang AZ, Langer R, Farokhzad OC. Nanoparticle delivery and cancer drugs. Annu Rev Med. 2012;63:185–98.
7. Hu CMJ, Zhang L. Nanoparticle-based combination therapy toward overcoming drug resistance in cancer. Biochem Pharmacol. 2012;83:1104–11.
8. Mora-Huertas CE, Garrigues O, Fessi H, Elaissari A. Nanocapsules prepared via nanoprecipitation and emulsification-diffusion methods: comparative study. Eur J Pharm Biopharm. 2012;80:235–9.
9. Liu Y, Wang W, Yang J, Zhou C, Sun J. pH-sensitive polymeric micelles triggered drug release for extracellular and intracellular drug targeting delivery. Asian J Pharm Sci. 2013;8:159–67.
10. Agarwal T, Gautham SN, Narayana H, Pal K, Pramanik K, Giri S, et al. Calcium alginate-carboxymethyl cellulose beads for colon-targeted drug delivery. Int J Biol Macromol. 2015;75:409–17.
11. Jo M, Park MH, Kollipara PS, An J, Song B, Han HS, et al. Anticancer effect of bee venom toxin and melittin in ovarian cancer cells through induction of death receptors and inhibition of JAK2/STAT3 pathway. Toxicol Appl Pharmacol. 2012;258:72–81.
12. Liu CC, Hau DJ, Zhang Q, An J, Zhao JJ, Chen B, et al. Application of bee venom and its main constituent melittin for cancer treatment. Cancer Chemother Pharmacol. 2016;78:1113–30.
13. Huh JE, Baek YH, Lee MH, Choi DY, Park DS, Lee JD. Bee venom inhibits tumor angiogenesis and metastasis by inhibiting tyrosine phosphorylation of VEGFR-2 in LL-tumor-bearing mice. Cancer Lett. 2010;292:98–110.
14. Gajski G, Garaj-Vrhovac V. Melittin: a lytic peptide with anticancer properties. Environ Toxicol Pharmacol. 2013;36:697–705.
15. Gao J, Xie C, Zhang M, Wei M, Yan Z, Ren Y, et al. RGD-modified lipid disks as drug carriers for tumor targeted drug delivery. Nanoscale. 2016;8:7209–16.
16. Leifer A, Lippincott ER. The infrared spectra of some amino acids. J Am Chem Soc. 1957;79:5098–101.
17. Imae T, Ikeda S. Infrared spectra and conformation of monodisperse oligo-γ-benzyl-L-glutamates in solution. Biopolymers. 1984;23:2573–86.
18. Venyaminov SY, Kalnin NN. Quantitative IR spectrophometry of peptide compounds in water solutions. I. Spectral parameters of amino acid residue absorption bands. Biopolymers. 1990;30:1243–57.
19. Bakker JM, Aleese LM, Meijer G, von Helden G. Fingerprint IR spectroscopy to probe amino acid conformations in the gas phase. Phys Rev Lett. 2003;91:203003.
20. Ito M, Imae T, Aoi K, Tsutsumiuchi K, Noda H, Okada M. In situ investigation of adlayer formation and adsorption kinetics of amphiphilic surface-block dendrimers on solid substrates. Langmuir. 2002;18:9757–64.
21. Ito M, Imae T. Self-assembled monolayer of carboxyl-terminated poly(amido amine) dendrimer. J Nanosci Nanotechnol. 2006;6:1667–72.
22. Yang JS, Ren HB, Xie YJ. Synthesis of amidic alginate derivatives and their application in microencapsulation of λ-cyhalothrin. Biomacromolecules. 2011;12:2982–7.
23. Mitamura K, Imae T, Saito N, Takai O. Fabrication and structure of alginate gel incorporating gold nanorods. J Phys Chem. 2008;112:416–22.
24. Azevedo MA, Bourbon AI, Vicente AA, Cerqueira MA. Alginate/chitosan nanoparticles for encapsulation and controlled release of vitamin B_2. Int J Biol Macromol. 2014;71:141–6.
25. Imae T, Okahashi K, Ikeda S. Structure of micelles formed by monodisperse hexa-(γ-benzyl-L-glutamate) in solution. Biopolymers. 1981;20:2553–66.
26. Imae T, Ikeda S. Proton magnetic resonance studies on conformation and association of oligo-γ-benzyl-L-glutamates in solution. Biopolymers. 1985;24:2381–402.
27. Xie HG, Li XX, Lv GJ, Xie WY, Zhu J, Luxbacher T, et al. Effect of surface wettability and charge on protein adsorption onto implantable alginate–chitosan–alginate microcapsule surfaces. J Biomed Mater Res. 2010;92A:1357–65.
28. Matai I, Gopinath P. Chemically cross-linked hybrid nanogels of alginate and PAMAM dendrimer as efficient anticancer drug delivery vehicles. Biomater Sci Eng. 2016;2:213–23.
29. Kayal S, Ramanujan RV. Doxorubicin loaded PVA coated iron oxide nanoparticles for targeted drug delivery. Mater Sci Eng C Mater Biol Appl. 2010;30:484–90.